

LncRNA MIR497HG inhibits proliferation and migration of retinal endothelial cells under high-level glucose treatment *via* miRNA-128-3p/SIRT1 axis

J. YANG¹, F.-J. YANG¹, Y.-G. WANG², G.-F. SU¹, X. MIAO¹

¹Department of Ophthalmology, The Second Hospital of Jilin University, Changchun, China

²Department of Cardiovascular Center, The First Hospital of Jilin University, Changchun, China

Abstract. – **OBJECTIVE:** The aim of this study was to elucidate the potential influence of MIR497HG on regulating proliferative capacity of human retinal endothelial cells (HRECs).

MATERIALS AND METHODS: Relative expression levels of MIR497HG, miRNA-128-3p (miRNA-128-3p) and SIRT1 in HRECs treated with different doses of glucose and mannitol were detected by quantitative Real Time-Polymerase Chain Reaction (qRT-PCR). Dual-Luciferase reporter gene assay was conducted to assess the interaction among MIR497HG, miRNA-128-3p, and SIRT1. In addition, the potential effects of MIR497HG/miRNA-128-3p/SIRT1 axis on proliferative and migratory capacities in HRECs were evaluated by Cell Counting Kit-8 (CCK-8), 5-Ethynyl-2'-deoxyuridine (EdU) and transwell assay, respectively.

RESULTS: High-level glucose (HG) treatment significantly downregulated MIR497HG and SIRT1 expression, whereas upregulated miRNA-128-3p expression in HRECs ($p < 0.05$). miRNA-128-3p was the target gene binding MIR497HG, and SIRT1 was the downstream gene of miRNA-128-3p. Overexpression of MIR497HG significantly attenuated proliferative and migratory abilities of HG-induced HRECs ($p < 0.05$). Furthermore, decreased trends were partially reversed by overexpression of miRNA-128-3p or knockdown of SIRT1.

CONCLUSIONS: MIR497HG is downregulated after HG treatment. In addition, it suppresses the proliferation and migration of HRECs by targeting miRNA-128-3p/SIRT1 axis, thus influencing the progression of diabetic retinopathy.

Key Words:

Diabetic retinopathy (DR), MIR497HG, miRNA-128-3p, SIRT1.

Introduction

Diabetes mellitus (DM) is a metabolic disease caused by insufficient insulin secretion and islet dys-

function. It is characterized by chronic, progressive elevation of blood sugar^{1,2}. A series of DM-induced pathological changes, including excessive production of ROS, inflammatory response and damage of blood vessels, may eventually result in diabetic microangiopathy^{3,4}. Diabetic retinopathy (DR) is a common vascular complication in DM patients, which is also the leading cause of DM-related blindness⁵.

In human genome, fewer than 2% of genes are able to encode proteins, the majority of which are non-coding sequences⁶. Long non-coding RNAs (lncRNAs) are a kind of non-coding RNAs with over 200 nucleotides in length. Abnormally expressed lncRNAs are closely associated with human diseases, including cardiovascular diseases and tumors⁷. Moreover, tissue-specific, dynamically regulated and abnormally expressed lncRNAs in T2DM are identified in human β cell transcriptome analysis⁸.

LncRNA MIR497HG is considered as a key lncRNA in ischemic stroke. In this paper, MIR497HG was found significantly downregulated after HG treatment. The aim of our study was to clarify the role of MIR497HG in DR, and to explore the potential molecular mechanism.

Materials and Methods

Cell Culture

Human retinal endothelial cells (HRECs) provided by American Type Culture Collection (ATCC; Manassas, VA, USA) were cultured in extracellular matrix (ECM) containing 10% fetal bovine serum (FBS; Gibco, Rockville, MD, USA), 100 U/mL penicillin and 100 μ g/mL streptomycin. When cultured to 90% of confluence, the cells were treated with different concentrations of glucose for 48 h.

Cell Transfection

In this study, pcDNA-MIR497HG, si-MIR497HG-1, si-MIR497HG-2, si-MIR497HG-3, miRNA-128-3p mimics, miRNA-128-3p inhibitor, si-SIRT1-1, si-SIRT1-2 and si-SIRT1-3 were provided by GenePharma (Shanghai, China). When cell density reached 70%, cell transfection was performed according to the instructions of Lipofectamine 2000 (Invitrogen, Carlsbad, CA, USA). Sequences of MIR497HG siRNAs were as follows: si-MIR497HG-1: 5'-GGAGAGGA-GAGGAGGAUCA-3'; si-MIR497HG-2: 5'-CAG-CAGAGGUCAUGAGAAG-3'; si-MIR497HG-3: 5'-GGUCAGAGGUGGAAGGCUC-3'.

Quantitative Real-Time Polymerase Chain Reaction (qRT-PCR)

TRIzol (Invitrogen, Carlsbad, CA, USA) reagent was applied for isolating cellular RNA. The concentration and purity of extracted RNA quantified using a spectrometer. Subsequently, extracted RNA was reversely transcribed into complementary deoxyribose nucleic acid (cDNA) using the PrimeScript RT reagent Kit (TaKaRa, Otsu, Shiga, Japan). SYBR Premix Ex TaqTM (TaKaRa, Otsu, Shiga, Japan) was utilized for qRT-PCR with the following conditions: at 95°C for 5 min, 40 cycles at 94°C for 10 s, 60°C for 45 s and 72°C for 30 s, followed by 68°C for 5 min and maintained at 4°C. Primer sequences used in this study were as follows: MIR497HG: F: 5'-ATAAGAATCCAGGTCGGGGC-3', R: 5'-CCCAAGGTTCCATCGTCCTC-3'; SIRT1: F: 5'-TAGCCTTGTCAGATAAGGAAGGA-3', R: 5'-ACAGCTTCACAGTCAACTTTGT-3'; GAPDH: F: 5'-CGCTCTCTGCTCCTCCTGTTC-3', R: 5'-ATCCGTTGACTCCGACCTTCAC-3'.

Cell Counting Kit-8 (CCK-8) Assay

Cells were first inoculated into 96-well plates at a density of 5×10^3 cells per well. At appointed time points, 10 μ L of CCK-8 solution (Dojindo Molecular Technologies, Kumamoto, Japan) was added in each well, followed by incubation at 37°C for 2 h in the dark. Absorbance at 450 nm was finally detected by a micro-plate reader.

5-Ethynyl-2'-Deoxyuridine (EdU) Assay

Cells were first inoculated into 96-well plates at a density of 1×10^3 cells per well. Subsequently, they were dyed with EdU solution (Invitrogen, Carlsbad, CA, USA) for 30 min and Hoechst 33342 for another 30 min in the dark. Images of EdU-positive cells, Hoechst-labeled nuclei and

their merged image were captured under a fluorescence microscopy.

Transwell Assay

Cells were first prepared into suspension with 2×10^5 cells/ml. 100 μ L of cell suspension was applied in the upper side of transwell chamber (Corning, Corning, NY, USA). Meanwhile, 500 μ L of medium containing 20% FBS was applied in the bottom side. After 48 h of incubation, cells migrated to the bottom side were fixed with methanol for 15 min and stained with crystal violet for 20 min. Migrating cells were observed under a microscope, and the number of migrated cells was finally counted.

Dual-Luciferase Reporter Gene Assay

Cells were first inoculated into 96-well plates at a density of 5×10^3 cells/well. Next, they were co-transfected with wild-type/mutant-type vectors and NC/miRNA-128-3p mimics/NC for 24 h. Afterwards, the cells were lysed and the supernatant was collected for detection of relative Luciferase activity.

Statistical Analysis

Statistical Product and Service Solutions (SPSS) 21.0 statistical software (IBM Corp., Armonk, NY, USA) was used for data analysis. GraphPad Prism 6.6 (La Jolla, CA, USA) was utilized for depicting figures. Experimental data were expressed as mean \pm SD (standard deviation). Paired two-tailed *t*-test was used to compare the differences between two groups. $p < 0.05$ was considered statistically significant.

Results

MIR497HG Protected Glycotoxic Damage of Retinal Endothelial Cells

HRECs were first treated with 5.5, 11, 25 or 30 mM glucose or mannitol (negative control) for 48 h. QRT-PCR data showed that MIR497HG was markedly downregulated after 25 mM or 30 mM glucose treatment ($p < 0.05$). However, mannitol treatment did not affect the expression level of MIR497HG ($p > 0.05$, Figure 1A). Transfection efficacy of pcDNA-MIR497HG in HRECs was verified by qRT-PCR (Figure 1B). After 48 h treatment of 30 mM glucose, the viability (Figure 1C) and EdU-positive ratio (Figure 1D) in HRECs were markedly enhanced ($p < 0.05$). However, this could be partially attenuated by overexpression

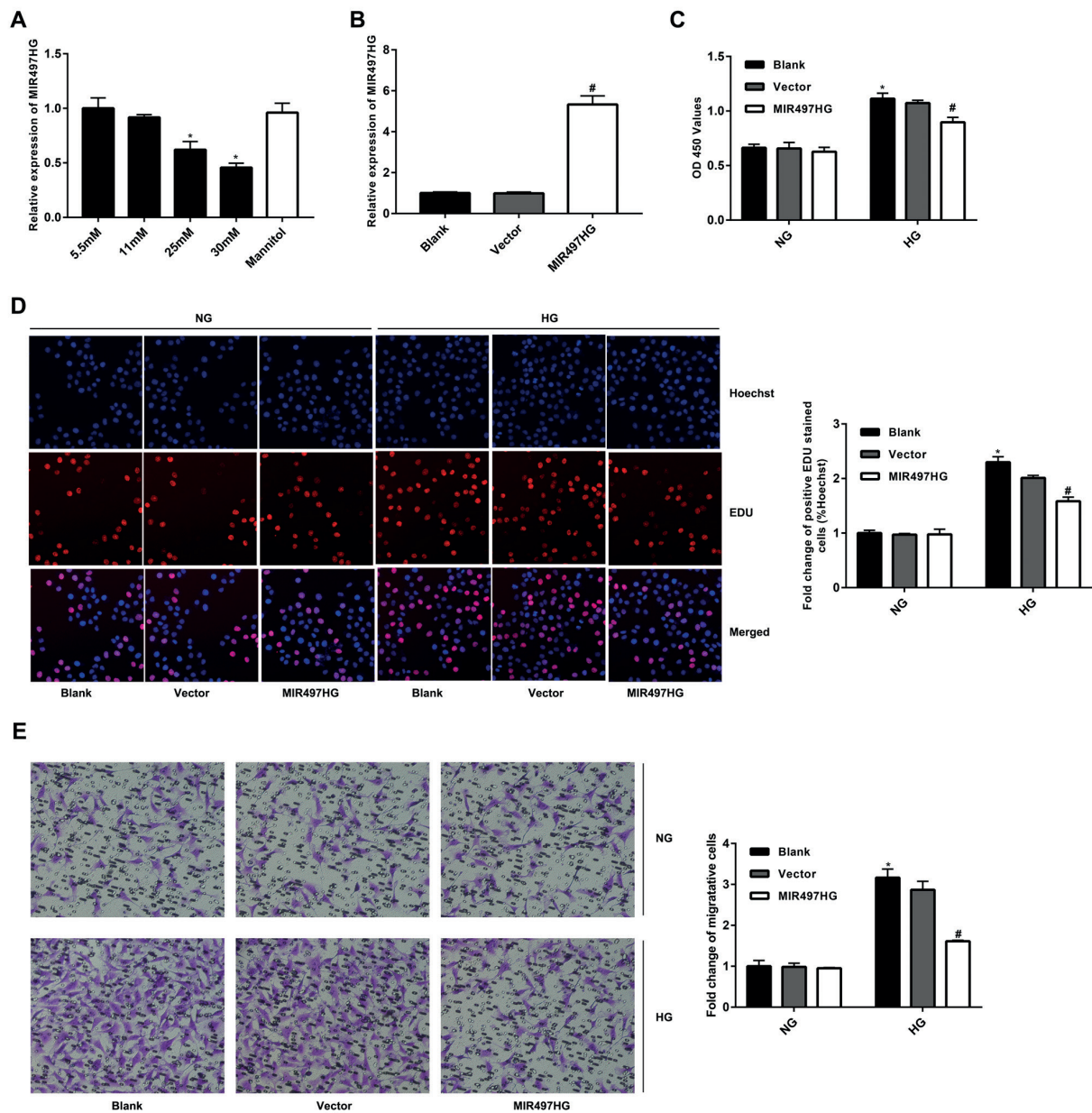


Figure 1. MIR497HG protected glycotoxic damage of retinal endothelial cells. **A**, MIR497HG level in HRECs treated with 5.5, 11, 25 or 30 mM glucose or mannitol (negative control) for 48 h. **B**, Transfection efficacy of pcDNA-MIR497HG in HRECs. **C**, Viability of NG-induced or HG-induced HRECs treated with blank control, vector or transfected with pcDNA-MIR497HG. **D**, EdU-positive ratio in NG-induced or HG-induced HRECs treated with blank control, vector or transfected with pcDNA-MIR497HG (magnification 40×). **E**, Migration of NG-induced or HG-induced HRECs treated with blank control, vector or transfected with pcDNA-MIR497HG (magnification 40×).

of MIR497HG. Similarly, HG-induced elevation in the migration of HRECs was abolished by transfection of pcDNA-MIR497HG (Figure 1E). Hence, MIR497HG was able to suppress the enhanced proliferative and migratory capacities in HG-induced HRECs.

MIR497HG Directly Bound MiRNA-128-3p

Potential binding sequences in 3'UTR of miRNA-128-3p and MIR497HG were predicted through bioinformatics method based on database, including TargetScan, microRNA and Diana Tools (Figure 2A). Subsequent results demon-

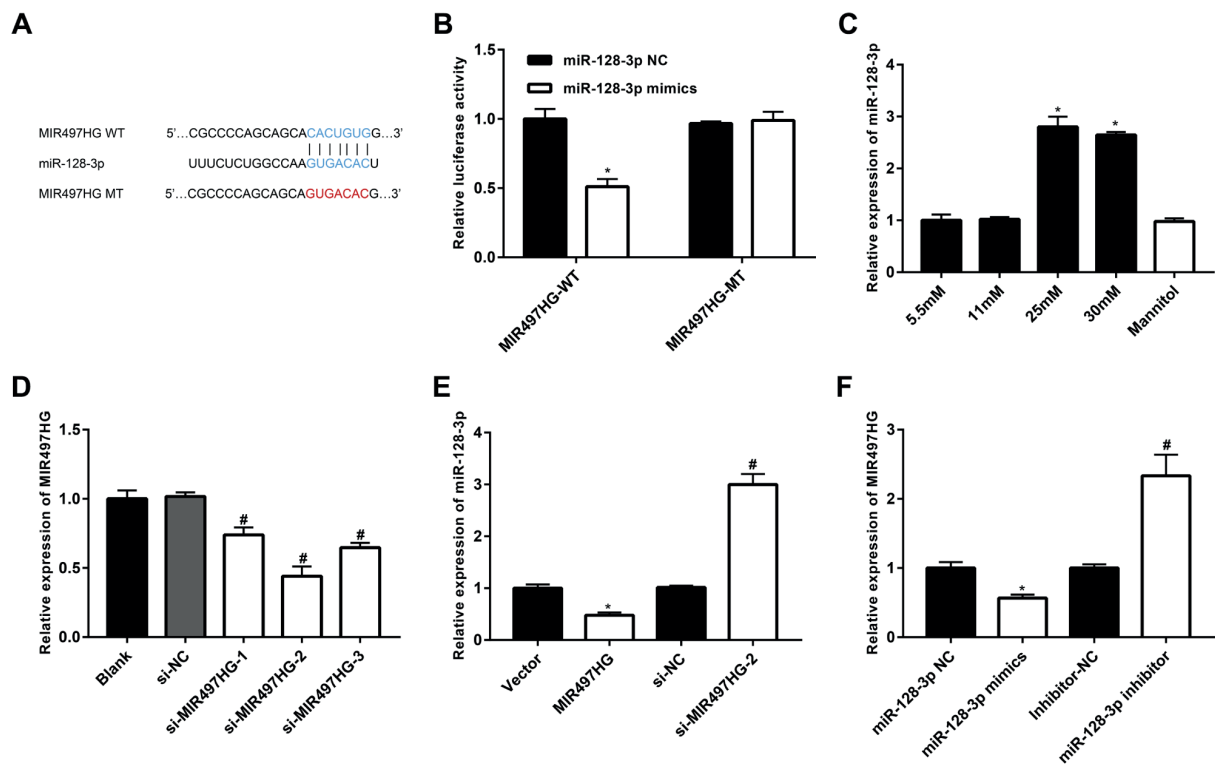


Figure 2. MIR497HG directly bound miRNA-128-3p. **A**, Binding sequences in 3'UTR of miRNA-128-3p and MIR497HG. **B**, Luciferase activity in HRECs co-transfected with MIR497HG-WT/MIR497HG-MUT and miR128-3p mimics/NC. **C**, MiRNA-128-3p level in HRECs treated with 5.5, 11, 25 or 30 mM glucose or mannitol (negative control) for 48 h. **D**, Transfection efficacy of three MIR497HG siRNAs in HRECs. **E**, MiRNA-128-3p level in HRECs transfected with pcDNA-MIR497HG or si-MIR497HG. **F**, MIR497HG level in HRECs transfected with miRNA-128-3p mimics or miRNA-128-3p inhibitor.

strated that luciferase activity was significantly reduced after co-transfection of MIR497HG-WT and miRNA-128-3p mimics ($p < 0.05$, Figure 2B). MiRNA-128-3p level was markedly upregulated after treatment of 25 or 30 mM glucose than those treated with mannitol ($p < 0.05$, Figure 2C). Subsequently, three MIR497HG siRNAs were constructed, and si-MIR497HG-2 presented the best transfection efficacy (Figure 2D). Transfection of pcDNA-MIR497HG remarkably downregulated miRNA-128-3p expression, whereas transfection of si-MIR497HG achieved the opposite trend in HRECs ($p < 0.05$, Figure 2E). Conversely, miRNA-128-3p negatively regulated MIR497HG expression level as well (Figure 2F).

SIRT1 Was the Downstream Gene of MiRNA-128-3p

In a similar way, SIRT1 was predicted to be the downstream gene binding miRNA-128-3p based on database, including TargetScan, microRNA and Diana Tools (Figure 3A). Co-transfection of SIRT1-

WT and miRNA-128-3p mimics remarkably quenched Luciferase activity ($p < 0.05$). However, Luciferase activity in SIRT1-MUT was unaffected ($p > 0.05$). This verified the binding relationship between miRNA-128-3p and SIRT1 (Figure 3B). The mRNA level of SIRT1 was significantly downregulated in HRECs treated with 25 or 30 mM HG for 48 h ($p < 0.05$, Figure 3C). Moreover, the overexpression of MIR497HG remarkably upregulated SIRT1 expression in HG-induced HRECs ($p < 0.05$, Figure 3D). On the contrary, miRNA-128-3p negatively regulated SIRT1 level (Figure 3E). Based on the above findings, it was considered that MIR497HG up-regulated SIRT1 in HRECs by sponging miRNA-128-3p.

MIR497HG/MiRNA-128-3p/SIRT1 Axis Regulated Proliferative Ability of HRECs

Among the three SIRT1 siRNAs, si-SIRT1-1 showed the best transfection efficacy. Therefore, it was selected for the following experiments (Figure 4A). Subsequent results revealed that de-

creased viability (Figure 4B), EdU-positive ratio (Figure 4C) and migratory cell number (Figure 4D) in HRECs overexpressing MIR497HG were partially reversed by overexpression of miRNA-128-3p or knockdown of SIRT1.

Discussion

DM is a highly prevalent chronic disease, which can be classified into T1DM, T2DM, gestational DM and others. Pathological changes owing to DM pose a great impact on human health^{9,10}. As a common vascular complication, DR is prevalent in DM patients with a relatively long disease course¹¹. DR is a risk factor for DM-related blindness; symptoms of DR in the early phase are mild, and obvious clinical manifestations are unobvious. Nevertheless, middle stage of advanced DR may lead to irreversible lesions. Meanwhile, there is still a lack of effective therapeutic strategies for DR. Therefore, it is important to intervene DR as early as possible. Currently, the pathogenesis of DR involves many factors. Apoptosis and loss of pericytes, microangioma formation and capillary

basement membrane thickening are the typical pathological features of DR¹².

So far, the critical functions of lncRNAs in vascular lesions have been highlighted¹³⁻¹⁹. There are 31 unknown lncRNAs discovered in human vascular smooth muscles through RNA sequencing. Knockdown of lncRNA SENCRC leads to the downregulation of a series of genes associated with contraction of myocardium and smooth muscle²⁰. Lnc-Ang362 is an AngII regulatory lncRNA, whose expression level affects the proliferative ability in vascular smooth muscle²¹. Silence of lncRNA MALAT1 regulates the proliferation and migration of vascular endothelial cells, thus attenuating angiogenesis²². Under the pathological condition of DM, MALAT1 mediates cellular functions of retinal endothelial cells by activating the p38/MAPK pathway²³. In this paper, MIR497HG was found significantly downregulated after high-level glucose treatment. Furthermore, overexpression of MIR497HG markedly suppressed the proliferative and migratory capacities of HRECs.

In recent years, the ceRNA mechanism of lncRNAs has been well concerned. A lncRNA sponges a corresponding miRNA, thereby af-

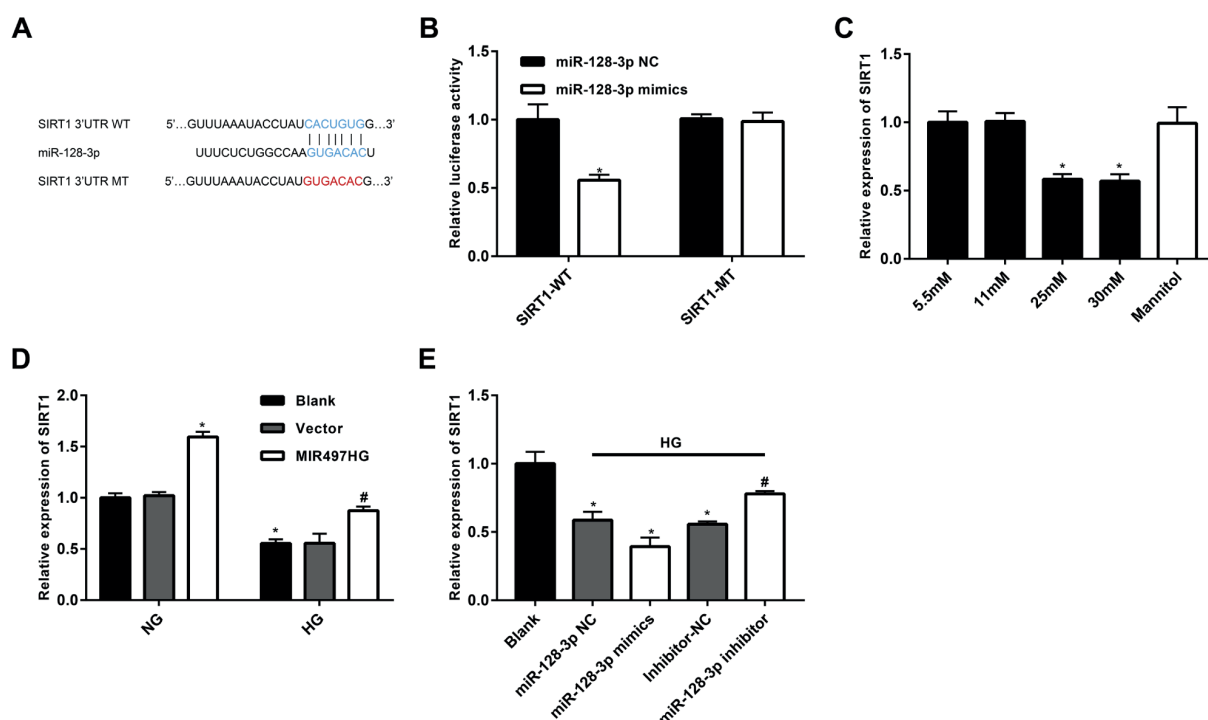


Figure 3. SIRT1 was the downstream gene of miRNA-128-3p. **A**, Binding sequences in the 3'UTR of SIRT1 and miRNA-128-3p. **B**, Luciferase activity in HRECs co-transfected with SIRT1-WT/SIRT1-MUT and miR128-3p mimics/NC. **C**, SIRT1 level in HRECs treated with 5.5, 11, 25 or 30 mM glucose or mannitol (negative control) for 48 h. **D**, SIRT1 level in NG-induced or HG-induced HRECs treated with blank control, vector or transfected with pcDNA-MIR497HG. **E**, SIRT1 level in HRECs transfected with miRNA-128-3p mimics or miRNA-128-3p inhibitor.

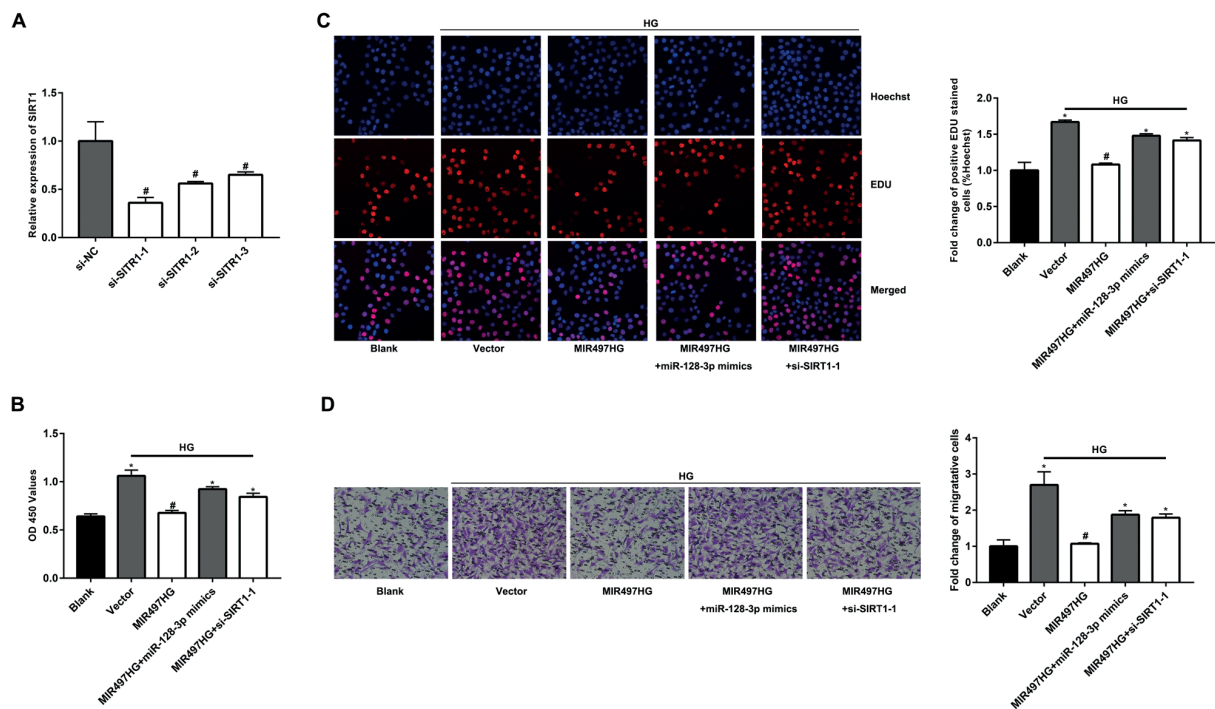


Figure 4. MIR497HG/miRNA-128-3p/SIRT1 axis regulated proliferative ability in HRECs. **A**, Transfection efficacy of three SIRT1 siRNAs. **B**, Viability in HRECs transfected with vector, pcDNA-MIR497HG, pcDNA-MIR497HG+miRNA-128-3p mimics or pcDNA-MIR497HG+si-SIRT1. **C**, EdU-positive ratio in HRECs transfected with vector, pcDNA-MIR497HG, pcDNA-MIR497HG+miRNA-128-3p mimics or pcDNA-MIR497HG+si-SIRT1 (magnification 40 \times). **D**, Migration of HRECs transfected with vector, pcDNA-MIR497HG, pcDNA-MIR497HG+miRNA-128-3p mimics or pcDNA-MIR497HG+si-SIRT1 (magnification 40 \times).

fecting its downstream gene expression²⁴. Our findings proved that MIR497HG sponged miRNA-128-3p to upregulate SIRT1. Importantly, MIR497HG/miRNA-128-3p/SIRT1 axis was responsible for regulating cellular phenotypes of HRECs, eventually influencing DR progression. *In vivo* experiments should be conducted to validate our findings in the near future. Moreover, the potential influence of MIR497HG on angiogenesis is required to be explored.

Conclusions

Taken together, MIR497HG is significantly downregulated after HG treatment. In addition, it suppresses proliferative and migratory abilities of HRECs bytargeting miRNA-128-3p/SIRT1 axis, eventually influencing DR progression.

Conflict of Interest

The Authors declare that they have no conflict of interests.

References

- XU Y, WANG L, HE J, BI Y, LI M, WANG T, WANG L, JIANG Y, DAI M, LU J, XU M, LI Y, HU N, LI J, MI S, CHEN CS, LI G, MU Y, ZHAO J, KONG L, CHEN J, LAI S, WANG W, ZHAO W, NING G. Prevalence and control of diabetes in Chinese adults. *JAMA* 2013; 310: 948-959.
- SEN S, CHAKRABORTY R. Treatment and diagnosis of diabetes mellitus and its complication: Advanced approaches. *Mini Rev Med Chem* 2015; 15: 1132-1133.
- LIEW G, WANG JJ, MITCHELL P. Retinopathy progression in type 2 diabetes. *N Engl J Med* 2010; 363: 2171-2172, 2173-2174.
- HAMMES HP, FENG Y, PFISTER F, BROWNLEE M. Diabetic retinopathy: targeting vasoregression. *Diabetes* 2011; 60: 9-16.
- RUNKLE EA, ANTONETTI DA. The blood-retinal barrier: structure and functional significance. *Methods Mol Biol* 2011; 686: 133-148.
- BALAKIREV ES, AYALA FJ. Pseudogenes: are they "junk" or functional DNA? *Annu Rev Genet* 2003; 37: 123-151.
- WAPINSKI O, CHANG HY. Long noncoding RNAs and human disease. *Trends Cell Biol* 2011; 21: 354-361.

- 8) MORAN I, AKERMAN I, VAN DE BUNT M, XIE R, BENAZRA M, NAMMO T, ARNES L, NAKIC N, GARCIA-HURTADO J, RODRIGUEZ-SEGUI S, PASQUALI L, SAUTY-COLACE C, BEUCHER A, SCHARFMANN R, VAN ARENSBERGEN J, JOHNSON PR, BERRY A, LEE C, HARKINS T, GMYR V, PATTOU F, KERR-CONTE J, PIEMONTI L, BERNEY T, HANLEY N, GLOYN AL, SUSSEL L, LANGMAN L, BRAYMAN KL, SANDER M, MCCARTHY MI, RAVASSARD P, FERRER J. Human beta cell transcriptome analysis uncovers lncRNAs that are tissue-specific, dynamically regulated, and abnormally expressed in type 2 diabetes. *Cell Metab* 2012; 16: 435-448.
- 9) BERG K, CLEMMENSEN TS, TRAM EM, KOEFOED-NIELSEN P, ILKJAER LB, POULSEN SH, EISKJAER H. Survival, graft function, and incidence of allograft vasculopathy in heart transplant patients receiving adverse risk profile donor hearts. *Clin Transplant* 2018; 32: e13343.
- 10) CARRAL-SANTANDER IE, SANTOS-PALACIOS A, MARTINEZ-BAEZ BE, CERNICHIARO-ESPINOSA L, ELIZONDO-CAMACHO JM, VALDES-LARA CA, MORALES-CANTON V, VELEZ-MONTOYA R. Secondary hyperhomocysteinemia-related occlusive retinal vasculopathy: a case report. *Am J Ophthalmol Case Rep* 2019; 13: 41-45.
- 11) YAU JW, ROGERS SL, KAWASAKI R, LAMOUREUX EL, KOWALSKI JW, BEK T, CHEN SJ, DEKKER JM, FLETCHER A, GRAUSLUND J, HAFFNER S, HAMMAN RF, IKRAM MK, KAYAMA T, KLEIN BE, KLEIN R, KRISHNAIAH S, MAYURASAKORN K, O'HARE JP, ORCHARD TJ, PORTA M, REMA M, ROY MS, SHARMA T, SHAW J, TAYLOR H, TIELSCH JM, VARMA R, WANG JJ, WANG N, WEST S, XU L, YASUDA M, ZHANG X, MITCHELL P, WONG TY. Global prevalence and major risk factors of diabetic retinopathy. *Diabetes Care* 2012; 35: 556-564.
- 12) ROBINSON R, BARATHI VA, CHAURASIA SS, WONG TY, KERN TS. Update on animal models of diabetic retinopathy: from molecular approaches to mice and higher mammals. *Dis Model Mech* 2012; 5: 444-456.
- 13) MAHMOUD AD, BALLANTYNE MD, MISCIANINOV V, PINEL K, HUNG J, SCANLON JP, IYINIKKEL J, KACZYNSKI J, TAVARES AS, BRADSHAW AC, MILLS NL, NEWBY DE, CAPORALI A, GOULD GW, GEORGE SJ, ULITSKY I, SLUIMER JC, RODOR J, BAKER AH. The human-specific and smooth muscle cell-enriched lncRNA SMILR promotes proliferation by regulating mitotic CENPF mRNA and drives cell-cycle progression which can be targeted to limit vascular remodeling. *Circ Res* 2019; 125: 535-551.
- 14) ZHANG M, WANG X, YAO J, QIU Z. Long non-coding RNA NEAT1 inhibits oxidative stress-induced vascular endothelial cell injury by activating the miR-181d-5p/CDKN3 axis. *Artif Cells Nanomed Biotechnol* 2019; 47: 3129-3137.
- 15) LI H, ZHU X, HU L, LI Q, MA J, YAN J. Loss of exosomal MALAT1 from ox-LDL-treated vascular endothelial cells induces maturation of dendritic cells in atherosclerosis development. *Cell Cycle* 2019; 18: 2255-2267.
- 16) KHYZHA N, KHOR M, DISTEFANO PV, WANG L, MATIC L, HEDIN U, WILSON MD, MAEGDEFESSEL L, FISH JE. Regulation of CCL2 expression in human vascular endothelial cells by a neighboring divergently transcribed long noncoding RNA. *Proc Natl Acad Sci U S A* 2019; 116: 16410-16419.
- 17) YANG L, LIANG H, SHEN L, GUAN Z, MENG X. LncRNA Tug1 involves in the pulmonary vascular remodeling in mice with hypoxic pulmonary hypertension via the microRNA-374c-mediated Foxc1. *Life Sci* 2019; 116769.
- 18) WANG D, XU H, WU B, JIANG S, PAN H, WANG R, CHEN J. Long noncoding RNA MALAT1 sponges miR1243p.1/KLF5 to promote pulmonary vascular remodeling and cell cycle progression of pulmonary artery hypertension. *Int J Mol Med* 2019; 44: 871-884.
- 19) HE X, ZHAO X, SU L, ZHAO B, MIAO J. MROH7-TTC4 read-through lncRNA suppresses vascular endothelial cell apoptosis and is upregulated by inhibition of ANXA7 GTPase activity. *FEBS J* 2019; 286: 4937-4950.
- 20) BELL RD, LONG X, LIN M, BERGMANN JH, NANDA V, COWAN SL, ZHOU Q, HAN Y, SPECTOR DL, ZHENG D, MIANO JM. Identification and initial functional characterization of a human vascular cell-enriched long noncoding RNA. *Arterioscler Thromb Vasc Biol* 2014; 34: 1249-1259.
- 21) LEUNG A, TRAC C, JIN W, LANTING L, AKBANY A, SAETROM P, SCHONES DE, NATARAJAN R. Novel long noncoding RNAs are regulated by angiotensin II in vascular smooth muscle cells. *Circ Res* 2013; 113: 266-278.
- 22) MICHALIK KM, YOU X, MANAVSKI Y, DODDABALLAPUR A, ZORNIG M, BRAUN T, JOHN D, PONOMAREVA Y, CHEN W, UCHIDA S, BOON RA, DIMMELER S. Long noncoding RNA MALAT1 regulates endothelial cell function and vessel growth. *Circ Res* 2014; 114: 1389-1397.
- 23) LIU JY, YAO J, LI XM, SONG YC, WANG XQ, LI YJ, YAN B, JIANG Q. Pathogenic role of lncRNA-MALAT1 in endothelial cell dysfunction in diabetes mellitus. *Cell Death Dis* 2014; 5: e1506.
- 24) LIN Z, LI X, ZHAN X, SUN L, GAO J, CAO Y, QIU H. Construction of competitive endogenous RNA network reveals regulatory role of long non-coding RNAs in type 2 diabetes mellitus. *J Cell Mol Med* 2017; 21: 3204-3213.